The granular fracture model for rock fragmentation

1991 J. Phys. A: Math. Gen. 24 L1175

(http://iopscience.iop.org/0305-4470/24/19/009)

J. Phys. A: Math. Gen. 24 (1991) L1175-L1184. Printed in the UK

LETTER TO THE EDITOR

The granular fracture model for rock fragmentation

Ury Naftaly†, Moshe Schwartz†, Amnon Aharony†‡ and Dietrich Stauffer†§

† School of Physics and Astronomy, Raymond and Beverly Sackler Faculty of Exact Sciences, Tel Aviv University, Tel Aviv 69978, Israel

‡ Department of Physics, University of Oslo, PO Box 1048 Blindern, N-0316 Oslo 3, Norway

§ Institut of Theoretical Physics, Cologne University, D-5000 Cologne 41, Federal Republic of Germany

Received 11 February 1991

Abstract. We introduce and study a model of granular fracture to mimic the dynamics of rock fragmentation. The model describes a rock as an assembly of interacting grains that evolve in time according to Newtonian dynamics. The main ingredient describing macroscopic rather than microscopic dynamics is a history-dependent attractive potential between pairs of grains, which is set to zero after the pair first moves beyond some threshold distance apart. We study the characteristics of the distribution of cluster sizes and compare them with the corresponding characteristics of the percolation problem. Our results show a decrease of the cluster numbers with sample size and an apparent breakdown of hyperscaling. We also find a dependence of critical exponents on the average initial kinetic energy of our system.

The characteristics of crack systems in rocks and the distribution of the sizes of the generated fragments is essential to many fields of science and technology. A few examples are oil recovery, mining and the strength of materials.

Mechanisms for the description of the formation and propagation of cracks range from continuous descriptions [1, 2] (in which it may be very difficult to obtain numerically the characteristics of a whole system of cracks) to lattice type descriptions [3-11]. In the latter one can find different approaches, from solution of the elastic equations for a single crack [3-4], through stress-dependent random generation of cracks (as in the random fuse model [5-7] or the kinetic breaking model [8-10]), to percolation descriptions of fracture [11]. The single crack models are not useful for describing an assembly of cracks. The percolation model assumes random formation of microcracks, while natural cracks in many cases are correlated. In the random fuse model or kinetic breaking model, the dynamics is artificial and imposes equilibrium on the system.

In the following we present a model that mimics the dynamics of natural fragmentation. The expectations of such a model are that it will dynamically introduce natural-looking correlations into the crack systems.

For real problems it is important to know not only what are the pieces of matter separated by cracks, i.e. the fragments, but also what is the geometry of the crack itself (e.g. its width as a function of its length, etc). Since the model presented here is described in a continuum, it might be possible to obtain (though not done here) additional geometrical information, beyond the information obtained on a lattice.

0305-4470/91/191175+10$03.50

In our model, the granular fracture model (GFM), a rock is described by an assembly of elementary building blocks. These building blocks represent macroscopic grains. In such a representation of a rock, we ignore cracks within the grains.

We assume now that the grains are spherical. The interaction between any two grains is basically a hard core one, described numerically by a scattering process once the distance between centres is the diameter of the grain, $R_{\min}$. In addition to that, we assume a continuous force which is responsible for the cohesion in the system. We assume that the force exerted by the jth on the ith grain is

$$F_{ij} = \begin{cases} \infty & \text{if } r_{ij} \leqslant R_{\min} \\ -[F_1(r_{ij} - R_0) - F_2(r_{ij} - R_0)^2]\hat{e}_{ij} & \text{if } R_{\min} < r_{ij} < R_{\max} \\ 0 & \text{otherwise} \end{cases} \tag{1}$$

where r_{ij} is the distance between the centres of the i and j grains, $\hat{e}_{ij}$ is a unit vector pointing from r_i to r_j, R_0 ($R_{\min} < R_0 < R_{\max}$) is the point where the force changes from repulsive to attractive, $R_{\max}$ is the point in which the force vanishes and F_1 and F_2 are constants. This force is assumed to act only between grains which were nearest neighbours on the initial lattice configuration, because it results from short-range interactions on the surface of the grains. Furthermore, it is history-dependent and it is set equal to zero for *all* later times once r_{ij} has increased beyond $R_{\max}$. The 'glue' property of the interaction represents the fact that once a macroscopic crack has been generated, closing it geometrically does not restore the attractive forces between the pieces.

We solve numerically Newton's equations of motion with the force described in (1), and apply a simple scattering procedure in which the velocities of the two scattered particles are exchanged when $r_{ij} = R_{\min}$. We assume that all the grains have the same mass and located at time $t = 0$ on a square 2D lattice with $r_{ij} = R_0$. The basic assumption here is that after some time randomization sets in, so that the initial square lattice (while important for numerical purposes, labelling, etc) will have no important effect on the structure of cracks at later times.

A real material is subject to the influence of external forces, that generate in turn some random velocities within the material. We take that into account by specifying a distribution of velocities from which the actual initial conditions are selected. We choose a uniform distribution with velocities $|\boldsymbol{v}| < v_0$, i.e.

$$p(\boldsymbol{v}) = (\pi v_0^2)^{-1}\Theta(v_0 - |\boldsymbol{v}|) \tag{2}$$

where v_0 is the cutoff velocity.

In the following, we use free boundary conditions. The dimensionless parameters used to obtain the results reported here are $F_1 = 50$, $F_2 = 100$, $R_{\max} = 1.1$, $R_{\min} = 1.0$, $R_0 = 1.05$. The mass m of a grain is taken to be 1.

The time step Δt in the numerical solution was chosen to obey

$$10 v_0 \Delta t \leqslant R_{\max} - R_{\min}. \tag{3}$$

The assembly of grains was evolved in time according to the procedure described above. In figure 1 we see a system of grains after 160 time steps, for $v_0 = 1$; one can see that there is a crack spanning the system. The first time such a crack is found is defined as the fracture time, t_c. All the results presented here were obtained when the systems of grains were detected to be at the fracture time.

Distribution of the number of clusters. We define a cluster of size s, as the assembly of s grains connected by a finite interaction at time t. We investigated the distribution of

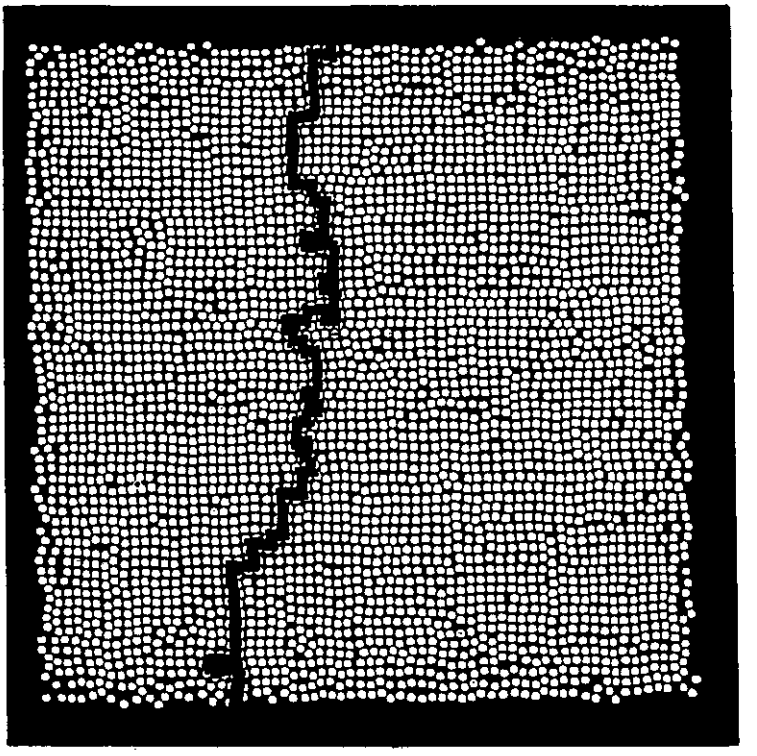

Figure 1. The positions of the grains (white circles) at the fracture time (here 160 time steps), for a 64×64 grains simulation. The cutoff velocity is 1. The crack spanning the system is emphasized by blackening half circles on both sides.

the number of clusters of size s per lattice site at the fracture time, $n_s(t_c)$, as a function of s. Since the number of large clusters in a finite sample is very small, statistics of large clusters is very hard to achieve in a reasonable number of simulations. Thus we collected the number of clusters of sizes $2^i \leqslant s < 2^{i+1}$, where i is an integer, into one number (this procedure is usually called 'binning' [12, 13]). The outcome of such a procedure on a power-law distribution will be an effective exponent which is larger by a unity. We define the number of clusters of sizes between 2^i and 2^{i+1} (the binned data) as

$$N_s(t_c) \equiv \sum_{s=2^i}^{s=2^{i+1}-1} n_s(t_c) \qquad \text{for } s = 2^{i+1}-1.$$

The results for $N_s(t_c)$ as a function of s for 95 systems of 64×64 grains with initial velocity $v_0 = 1$, on a log–log plot, is shown in figure 2. It seems that a power-law behaviour of the kind

$$N_s(t_c) \propto s^{-(\tau-1)} \tag{4}$$

describes the behaviour of n_s relatively well up to cluster sizes of $\frac{1}{8}$ to $\frac{1}{4}$ of the system mass. There the number of clusters is much larger than expected according to (4). The slope in figure 2 gives the exponent $-(\tau-1)$ in equation (4). The result for τ as thus obtained using only statistical error and taking into account only the points from $s = 3$

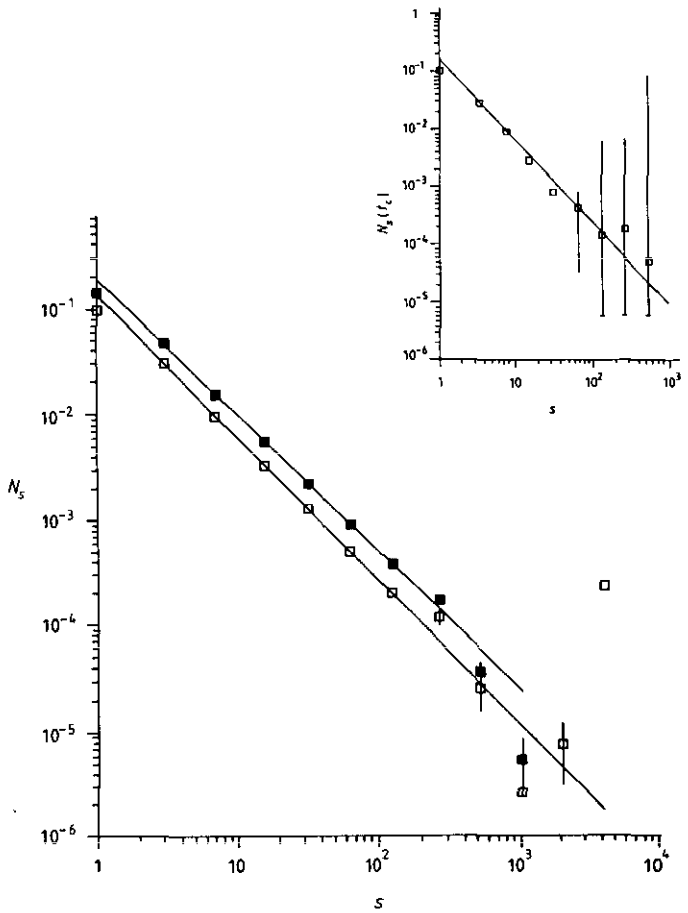

Figure 2. The binned number of clusters of size s per lattice site, N_s as a function of s for a 64×64 system (open squares), and the partial sums (7) as a function of s for the same system (full squares). The result of the extrapolation to infinite lattice sizes of N_s as a function of s are shown in the upper corner. The cut error bars denote very big errors that, due to least-squares fit have only a small influence on the line. In all the graphs the error bars are purely statistical and $v_0 = 1$.

to $s = 1023$ is

$$\tau - 1 = 1.35 \pm 0.01. \tag{5}$$

In order to compare this to the uncorrelated percolation exponent we performed the same procedure on 100 bond-percolating systems of 64×64 nodes in each. The probability of a bond to be broken in the percolating systems was the same as the average probability for a bond to be broken in the dynamic systems as was measured at the fracture time, t_c, which turned out to be equal to the bond percolation threshold of a square lattice, $p_c = 0.5$ within the statistical error. When a graph similar to that in figure 2 was plotted, a different exponent of

$$\tau - 1 = 0.989 \pm 0.007 \tag{6}$$

was found. This value differs from the theoretical percolation value $\frac{187}{91}$ [14, 15]. (The difference is due to finite size effects [16].)

Comparing our system to percolation at the large clusters, we see a striking difference. Out of 100 percolating systems at fracture concentration, 28 clusters of size $s > 2047$ were found. In contrast, 92 such clusters were found in the 95 dynamic systems. On the other hand, 54 clusters of size $511 < s < 1024$ were found in the percolation systems, while only 1 was found in the 95 dynamical systems at t_c.

The exponent τ obtained for our system is found to be significantly different from that of percolation. We first checked whether this is not a spurious result originating in the procedure of analysis. Two sources that may lead to a deviation in the calculated τ are the binning procedure and the finite size of the system.

To check the effect of the binning procedure on the GFM exponent, we computed the partial sums

$$\sum_{s' \geqslant s}^{\infty} n_{s'}(t_c) \tag{7}$$

for the GFM clusters. One can easily show [13] that the result scales as $s^{-(\tau-1)}$, independent of the binning procedure, since there is a summation in (7). The partial sums (7) are shown is figure 2 for 130 simulations, 64×64 grains with initial velocity 1 in each. The slope is

$$\tau - 1 = 1.293 \pm 0.006. \tag{8}$$

In order to obtain the behaviour of the GFM systems for L infinite, we calculated $N_s(t_c)$ for different sizes of systems, varying from $L = 10$ to $L = 78$, where L is the linear size of the initial lattice of grains. A linear extrapolation of $N_s(t_c)$ as a function of $1/L$ was then used to estimate the value of $N_s(t_c)$ for $L \to \infty$. The results of N_s achieved this way are plotted on a log–log plot in figure 2 as a function of s. The slope in this graph is

$$\tau - 1 = 1.4 \pm 0.02. \tag{9}$$

Both checks strongly suggest that τ for percolation and for GFM are indeed different.

The fractal dimension. In order to compare the fractal dimension [17] of percolation with that of the GFM we computed the latter while using the position of the grains on the initial lattice. To get the fractal dimension, we computed the average radius of gyration [18] of the clusters at a given bin, R_s. If the clusters are fractal, then the mass, M (or number of grains) of a cluster will be proportional to its radius to a fractional power, that is

$$M_s \propto R_s^D \tag{10}$$

when D is defined as the fractal dimension.

The results for R_s, for different sizes of systems and different initial velocities are plotted in figure 3. One can see, however, that the data from the different systems sit on the same curve. That implies that the fractal dimension of the GFM systems does not change much with the variation of the parameters of the model. This result may change if we examine the fractal dimension of the clusters using the real positions of the grains. The slope of the line in figure 3 was found to be:

$$1/D = 0.52 \pm 0.02 \tag{11}$$

and thus

$$D = 1.92 \pm 0.07. \tag{12}$$

This result is very close to the percolation result $D = \frac{91}{48}$ [14, 15].

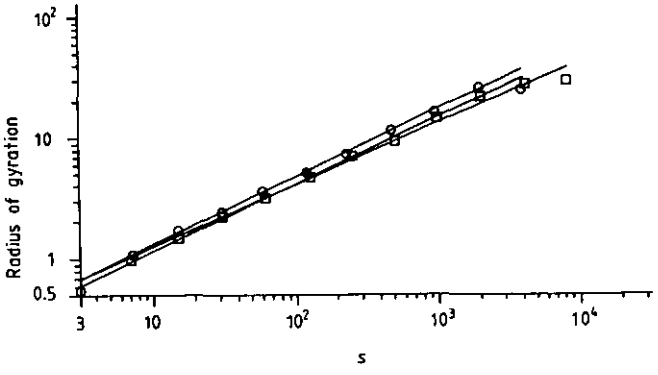

Figure 3. The radius of gyration as a function of s for different systems: $L=78$ and $v_0=1$ (open squares), $L=64$ and $v_0=1.2$ (crossed squares), and $L=64$ and $v_0=0.6$ (circles).

Dependence on the velocity cutoff. The question arises whether the results reported so far will remain the same as we change the parameters of the model. To examine this question we repeated the simulations discussed above for cutoff velocities different than 1. In figure 4 one can see the behaviour of the exponent $\tau-1$ as a function of the cutoff velocity. τ peaks around $v_0=1$, going over to the percolation value at very large and very small v_0. The behaviour of τ in the high initial velocity regime is clear. Since the velocities of the grains are large, the effect of the interaction between them is negligible and thus, since the distribution of the velocities is random, the breaking of the bonds is percolative. Such behaviour may be found in other physical processes, e.g. atomic nuclei break into lighter nuclei when hit by energetic projectiles [19]. The other parts of the graph in figure 4 are still not understood.

In order to find whether the GFM systems show the same behaviour for different L, we plotted $N_s(t_c)$ for systems of $L=64$ and $L=32$ on the same plot. Scaling requires

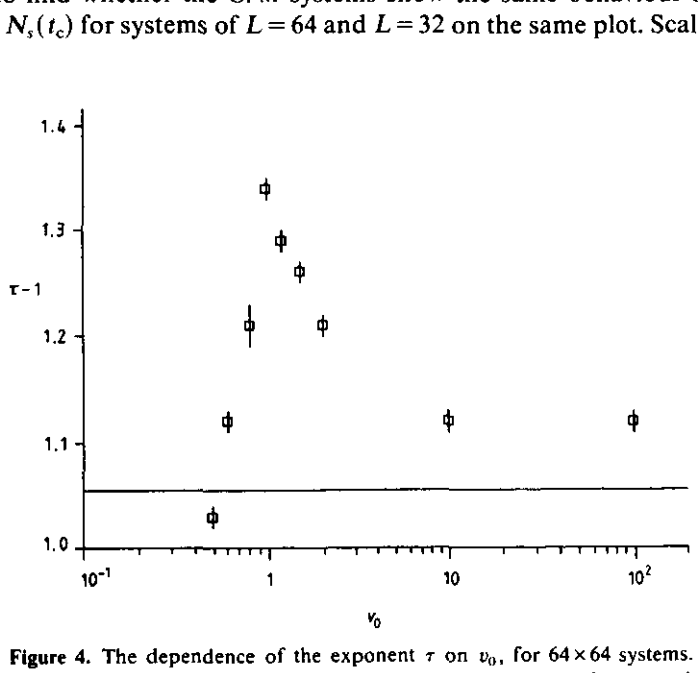

Figure 4. The dependence of the exponent τ on v_0, for 64×64 systems. The solid line represents the percolation value. The scale is half-logarithmic for convenience.

the data to overlap (data collapse) if the appropriate scaling exponents are used. In figure 5 we obtained data collapse in the form:

$$N_s(L) \propto L^{-B} f(s/L^A) \tag{13}$$

where $A = 1.9$ and $B = 2.76$. Using (10) and (12) the exponent A can be identified as the fractal dimension D.

At criticality, equation (4) showed that $N_s \propto s^{-(\tau-1)}$. Equation (13) is consistent with that behaviour only if the function f behaves (for small x) as $f(x) \propto x^{-(\tau-1)}$, implying that

$$N_s(L) \propto L^{-\theta} s^{-(\tau-1)} \tag{14}$$

with $\theta = B - D(\tau - 1)$. Using $\tau - 1 \simeq 1.35 \pm 0.05$, $D \simeq 1.9$ and $B \simeq 2.76$ we find

$$\theta \simeq 0.2 \pm 0.1. \tag{15}$$

Scaling thus requires that, unlike in percolation, the amplitude q_0 of the cluster numbers, $N_s = q_0(L) s^{1-\tau}$ depends on L. This is probably due to the fact that the largest cluster grows with L, causing a decrease in the small cluster numbers.

Equation (14) implies that $N_s(L)$ may be written as a one-variable function

$$N_s(L) \equiv f(z) \propto z^{-(\tau-1)} \tag{16}$$

where $z \equiv sL^{\theta/(\tau-1)}$. In figure 6 we plot $N_s(L)$ against z on a log-log plot. The slope of the line is 1.293 ± 0.005, which agrees with (5). In order to get the best data collapse

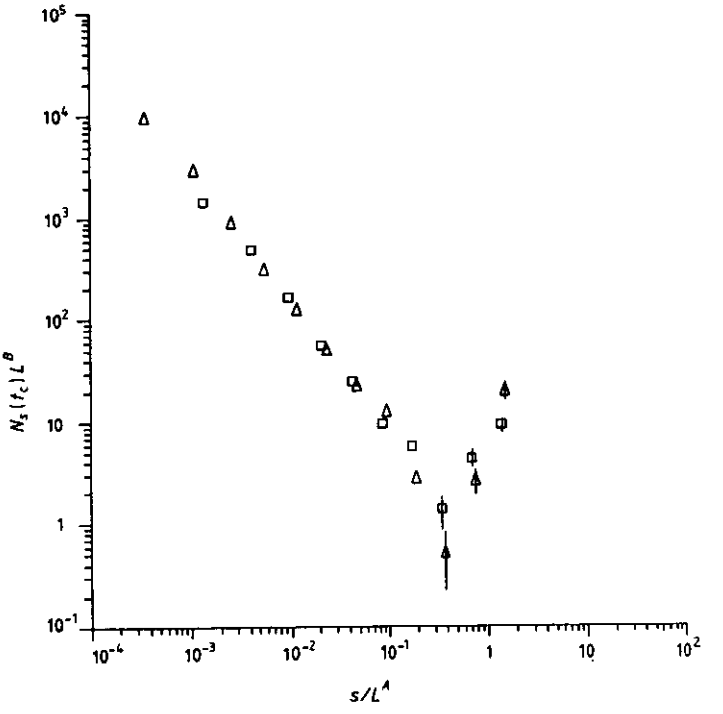

Figure 5. Data collapse of N_s for 64×64 and 32×32 systems with $v_0 = 1$, with exponents $A = 1.9$ and $B = 2.76$.

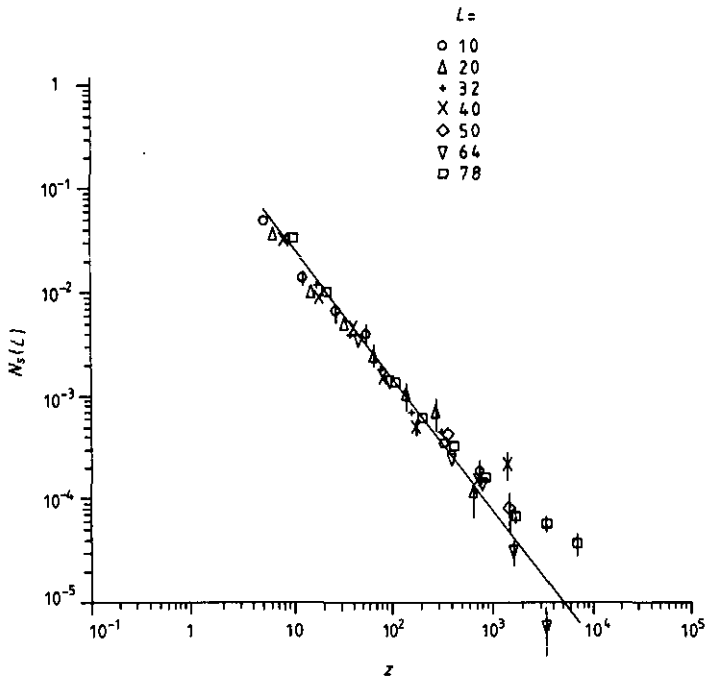

Figure 6. Data collapse of N_s (equation (16)) for different system sizes, for $P = 0.29$ and $v_0 = 1$. Only the decreasing part of N_s is used, and the points for $s = 1$ are omitted.

we used different values for the exponent $P \equiv \theta/(\tau - 1)$. We obtained the best data collapse using $P = 0.29$, which gives

$$\theta \simeq 0.37. \tag{17}$$

Another way to get θ is to plot the amplitude $q_0 = s^{\tau-1}N(s, L)$ for a specific s against L. Doing that, we observe a qualitative decrease of q_0 as a function of L. However, the data were not sufficiently accurate to yield an estimate for θ.

We thus see that the GFM cluster numbers obey normal scaling. The situation is more complicated with hyperscaling. In percolation, one has the hyperscaling relation

$$\tau = \frac{D + d}{D}. \tag{18}$$

In percolation, this relation results from the fact that

$$N_s(L) \propto s^{-(\tau-1)} \propto L^{-d}\left(\frac{s}{L^D}\right)^{-(\tau-1)} \tag{19}$$

and the prefactor L^{-d} comes from the fact that N_s scales like a density of points in the full Euclidean sample [20]. A comparison between (13) and (19) shows that the hyperscaling law (19) would hold only if we had $B = d$. The fact that $B > d$ again reflects the decrease of the total number of small clusters due to the fast increase of the largest cluster. Thus, hyperscaling is broken.

A breakdown of hyperscaling also occurs for percolation in dimensions $d > 6$ [20]. There it happens due to the appearance of a 'dangerous irrelevant variable' w, [20] so

that

$$N_s(L) = L^{-d} f\left(\frac{s}{L^D}, wL^{\omega}\right). \tag{20}$$

The function $f(x, y)$ is singular in y, $f(x, y) \propto y^{-\kappa}$, so that we end up with

$$N_s(L) \propto L^{-d-\kappa\omega} w^{-\kappa} \left(\frac{s}{L^D}\right)^{-(\tau-1)} \tag{21}$$

and thus, in the case here: $B = d + \kappa\omega$ and $\kappa\omega \approx 0.76$. At present we have no direct explanation of the new variable w for our fracture model.

To summarize, we have introduced the GFM in order to mimic fragmentation of rock. The analysis of the fragments at t_c, the time where a first crack goes through the system, can be done in an analogous way to the procedures used in percolation. The results for the critical exponents are different from those for percolation. Scaling holds, but requires a dependence of n_s on the size of the system, while hyperscaling is broken. We find also that the exponents depend on the kinetic energy per particle (the cutoff velocity) in the system, and the most marked departure from percolation occurs around $v_0 = 1$. At the present stage it is not clear, whether indeed there is a continuous dependence of the exponents on v_0 or whether, like in phase transitions, we see just effective exponents, resulting from a crossover between the percolation exponents valid for almost all v_0, to some special exponents at the isolated point $v_0 \approx 1$.

The work at the Tel Aviv University was supported by the Israel Academy of Sciences and by the US-Israel Binational Science Foundation. The work at the University of Oslo has been supported by VISTA, a research cooperation between the Norwegian Academy of Science and Letters and Den norske stats oljeselskap a.s. (STATOIL), by the Norwegian Council of Science and Humanities (NAVF) and by the Norwegian German Research Corporation. D Stauffer acknowledges partial support from BMFT grant 0326657D. U Naftaly thanks H J Herrmann, P Meakin, B B Mandelbrot and R Blumenfeld for helpful discussions.

References

[1] Griffith A A 1920 *Phil. Trans. R. Soc.* A **221** 163
[2] Johnson C 1987 *Numerical Solution of Partial Differential Equations by the Finite Element Method* (Cambridge: Cambridge University Press)
For application see for example:
Wellman G W, Rolfe S T and Dodds R H 1985 *Fracture Mechanics: Sixteenth Symposium* ed M F Kannimen and A T Hopper (Philadelphia, PA: ASTM) p 214
[3] Louis E, Guinea F and Flores F 1986 *Fractals in Physics* ed L Pietronero and E Tosatti (Amsterdam: Elsevier) p 177
[4] Louis E and Guinea F 1987 *Europhys. Lett.* **3** 871
[5] de Arcangelis L, Redner S and Herrmann H J 1985 *J. Physique Lett.* **46** L585
[6] Takayasu H 1986 *Fractals in Physics* ed L Pietronero and E Tosatti (Amsterdam: Elsevier) p 181
[7] Kahng B, Batrouni G G, Redner S, de Arcangelis L and Herrmann H J 1988 *Phys. Rev.* B **37** 7625
[8] Termomia Y and Meakin P 1986 *Nature* **320** 429
[9] Herrmann H J, Hansen A and Roux S 1989 *Phys. Rev.* B **39** 637
[10] Skjeltorp A T and Meakin P 1988 *Nature* **335** 424
[11] Aharony A 1986 *Fragmentation Form and Flow in Fractured Media (Annals Israel Physical Society 8)* ed R Englman and Z Jaeger (Bristol: Adam Hilger) p 74
[12] Quinn G D, Bishop G M and Harrison R J 1976 *J. Phys. A: Math. Gen.* **9** L9

[13] Margolina A, Nakanishi H, Stauffer D and Stanley H E 1984 *J. Phys. A: Math. Gen.* **17** 1683
[14] den Nijs M P M 1979 *J. Phys. A: Math. Gen.* **12** 1857
[15] Pearson R B 1980 *Phys. Rev.* B **22** 2579
[16] Rapaport D C 1985 *J. Phys. A: Math. Gen.* **18** L175
[17] Mandelbrot B B 1977 *Fractals: Form, Chance and Dimension* (San Francisco: Freeman)
[18] Stauffer D 1979 *Phys. Rep.* **54** 1
[19] Campi X 1986 *J. Phys. A: Math. Gen.* **19** L917
[20] Aharony A 1986 *Directions in Condensed Matter Physics* ed G Grinstein and G Mazernko (Singapore: World Scientific) p 1